Møller–Plesset Perturbation Energies and Distances for HeC_{20} Extrapolated to the Complete Basis Set Limit

A. J. C. VARANDAS

Departamento de Química, Universidade de Coimbra, 3004-535 Coimbra, Portugal

Abstract: The potential energy surface for the C_{20}–He interaction is extrapolated for three representative cuts to the complete basis set limit using second-order Møller–Plesset perturbation calculations with correlation consistent basis sets up to the doubly augmented variety. The results both with and without counterpoise correction show consistency with each other, supporting that extrapolation without such a correction provides a reliable scheme to elude the basis-set-superposition error. Converged attributes are obtained for the C_{20}–He interaction, which are used to predict the fullerene dimer ones. Time requirements show that the method can be drastically more economical than the counterpoise procedure and even competitive with Kohn-Sham density functional theory for the title system.

© 2008 Wiley Periodicals, Inc.   J Comput Chem 00: 000–000, 2008

Key words: HeC_{20}; MP2 calculations; CBS extrapolation

Introduction

Van der Waals (vdW) interactions are well known in nature. In particular, the simplest fullerene-helium interaction (exohedral HeC_{20}) can be representative of elusive systems with primary interest in gas and condensed phases of nanoscopic systems while presenting a particularly severe test both to molecular orbital[1] (MO) methods and density functional theory[2,3] (DFT). Although the latter dominates at present much of electronic structure calculations in condensed physics and quantum chemistry due to its rapid speed and surprising accuracy, it has also notable failures some of which will be pointed out later. In this work, we study the He $\cdots C_{20}$ interaction using an *ab initio* MO scheme that has been used thus far only for small systems.

With $V = 20$ vertices, $E = 30$ edges, and $F = 12$ faces (all pentagonal), dodecahedral C_{20} forms a closed $3D$ carbon cage obeying the rule $\mathcal{C} = V - E + F$ where $\mathcal{C} = 2$ is Euler's characteristic number for simple polyhedra. This dodecahedral-cage cluster has been synthesized,[4–7] and its existence in gas phase confirmed,[4] being the smallest possible fullerene cage.[8] Many theoretical articles have appeared in the literature on C_{20} over the past decade or so (refs. 9, 10, and references therein) with correlated *ab initio* calculations predicting the above structure for the ground state conformer. Of them, all electron calculations[11] using coupled-cluster singles and doubles theory with a perturbational estimate of connected triple excitations [CCSD(T)] and a double-zeta correlation consistent basis set of Dunning's[12] cc-pVXZ variety ($X = D : 2, T : 3, Q : 4, \ldots$ is the cardinal number) favor the above fullerene cage over the bowl or ring isomers. In turn, second-order

Møller–Plesset perturbation theory (MP2) calculations using a large polarized valence triple-zeta basis set suggest that the cage and bowl are almost isoenergetic,[13] a conclusion similar to the one reached by more recent DFT and MP2 calculations.[10,14,15] However, the bowl-cage-ring energy ordering seems to be preferred when going to higher levels of MP perturbation theory (MP4) or CCSD(T) calculations using different basis sets.[10] Additionally, quantum Monte Carlo suggests a bowl-ring-cage ordering.[16] Although the relative stability issue is still an open one, it will not be pursued here. Because the cage form is common to the larger members of the fullerene family that we envisage to study, dodecahedral C_{20} stands as the simplest representative on which our approach can be tested.

Computational studies to assist the characterization of C_{20} are also numerous (refs. 7, 9, 14 and references therein), covering from chemical reactivity[17] to molecular dynamics simulations of C_{20} and its chemisorption on surfaces,[18] just to mention a few. Notably, dodecahedral C_{20} seems to retain its shape in collisions,[18,19] suggesting a memory effect analogous to that observed when forming films.[20] Thus, despite its fleeting existence in condensed states, this may also support our choice of dodecahedral C_{20} as the smallest fullerene (structure taken from Ref. 21) and investigate its interaction with the smallest inert gas atom. Although the calculated

energies may be used for studying the scattering of dodecahedral C_{20} with helium, they will be used here to predict a potential for the weak interaction involving two such orientationally disordered fullerenes, which may be of help on investigations of the corresponding fullerite and its equilibrium with the gaseous phase. Jahn–Teller distortions of dodecahedral C_{20} will be ignored,[15,22] but the number of electrons and size disparity ensure enough challenge.

Theoretically, vdW interactions must be calculated with electronic structure methods that warrant size consistency.[23] This is satisfied by both the Hartree–Fock (HF) and MP2 methods used in this work. In turn, DFT is the popular route for calculations on large molecular systems, because it includes correlation and involves an effort similar to that required for an HF calculation, particularly when using hybrid methods.[24] In fact, with an expansion of the orbitals in basis functions, the number of integrals for solving the Kohn–Sham[2,3] equations scale as the fourth power of the number of such functions (M^4), thus in a way formally similar to HF theory. However, weak interactions due to dispersion (vdW type) are known to be poorly described by current functionals.[25] Although the local density approximation method seems to predict an attraction between, for example, rare gas atoms, essentially all gradient corrected methods predict a purely repulsive interaction.[24] Recent developments appear to be successful but still require empirical dispersion corrections.[26–28] Also successful in overcoming the drawbacks of DFT in the study of weak interactions seem to be methods that consider its linear response extension in the time domain to excited states, so-called TDDFT.[29] In this work, we make no attempt to pick a functional from the plethora of existing ones as any choice would not be free from arbitrariness. Indeed, DFT will only be invoked to assess computational costs. Regarding MP2 theory, it is known[24] to account typically for 80–90% of the correlation energy, with the first-order correction being the HF energy. Although MP2 is formally a M^5 method, it is the most economical MO approach for including electron correlation, an asset for selection in this work. Of course, for cost reasons that will become obvious later, we leave aside the problem of convergence of the perturbation expansion. Suffice it to say that convergence is often assumed to depend on the dominance of the single configuration reference, although the nature of convergence seems to be more complicated and even change (leading typically to a slower convergence) by basis set extension to include diffuse functions.[30]

It is well established that a major difficulty in the calculation of weakly bound interactions arises due to the use of finite sets of basis functions. This makes the description of the complex and the fragments unbalanced leading to a spurious attraction known as the basis set superposition error[1,31–36] (BSSE). The popular remedy to this error is the counterpoise (CP) method of Boys and Bernardi,[37] where the monomer energies are calculated with the full dimer basis. Recently, we suggested[38] that the BSSE may be eluded by extrapolating the raw energies without CP (NCP) to the complete basis set (CBS) limit; for a similar conclusion on thermochemistry calculations that has recently come to our attention, see ref. 39. The success should, however, be viewed with care as HF interaction energies (CP and NCP) have been found[32] to converge unsystematically for weakly interacting systems studied using correlated consistent basis sets[12] of the VXZ type, with a similar trend being observed for the NCP correlation contribution. Halkier et al.[32] attributed this result to the presence of both BSSE and the error due to an incomplete

description of the electronic Coulomb cusp. They gathered that once the former effect is removed by CP, the cusp dominates and convergence of the CP correlation contribution follows a X^{-3} form similar to the correlation energy. If both CP and CBS turn out to be mandatory, then an accurate description of weak interactions[32,34] will require a huge effort as six molecular calculations per geometry will at least be required. On the other hand, Schwenke and Truhlar[40] noted that inclusion of the CP correction may not warrant by itself an improved potential. Because our previous work on the helium dimer[38] has shown that CBS extrapolation may be all that is required, it will be worth investigating on a larger system whether a similar conclusion applies. This will also be studied here for the C_{20}... He interaction, with the results being found to corroborate that CBS extrapolation without CP suffices to obtain an accurate PES for weakly bound systems. Of course, this work will simultaneously provide a test of our scheme to CBS extrapolate the correlation energy, which had been used thus far only for small molecular systems. The calculated energies will be given in hartree and the binding energies in electronvolts (1 E_h = 27.211385 eV).

The structure of the work is as follows. Theory and Computational Methodology describes the basic theory and computational methodology, whereas the results are reported in Results and Discussion. Some conclusions regarding the potential of the method are explained in the final section.

Theory and Computational Methodology

As usual, the total energy is split into its HF and correlation (cor) parts: $E_X^{AB}(R) = E_X^{AB,HF}(R) + E_X^{AB,cor}(R)$, where X has the meaning previously assigned. Traditionally, for the AB system, the interaction energy assumes the form

$$\Delta E_X^{AB}(R) = \sum_\kappa \Delta E_X^{AB,\kappa}(R) \qquad (1)$$

where

$$\Delta E_X^{AB,\kappa}(R) = E_X^{AB,\kappa}(R) - E_X^{A,\kappa} - E_X^{B,\kappa} \qquad (2)$$

and the summation in eq. (1) runs over the κ = HF and cor components. The fragment energies are therefore calculated in their own basis and the energy of the complex in the combined basis of the fragments.

An approximate way to overcome BSSE is by using the CP-corrected[31,37] interaction energy

$$\Delta E_{CP,X}^{AB}(R) = \sum_\kappa \Delta E_{CP,X}^{AB,\kappa}(R) \qquad (3)$$

where

$$\Delta E_{CP,X}^{AB,\kappa}(R) = E_X^{AB,\kappa}(R) - E_X^{AQ,\kappa}(R) - E_X^{BQ,\kappa}(R) \qquad (4)$$

and Q is the ghost of species A or B. The energies to CBS extrapolate are then $E_X^{A\tilde{B},\kappa}(R)$ at NCP level and also $E_X^{AQ,\kappa}(R)$ and $E_X^{BQ,\kappa}(R)$ at CP.

CBS extrapolations have been inferred from the dependence of the correlation energy on the partial wave quantum number for two-electron atomic systems and second-order pair energies in many-electron atoms,[41,42] with a popular rule (a more extensive list of references can be found elsewhere[43,44]) being[45] $E_X^{cor} = E_\infty^{cor} + A_3/(X+\alpha)^3$, where E_X^{cor} is the correlation energy for basis set of cardinal number X, and E_∞^{cor} and A_3 are parameters determined from calculations for the two highest affordable values of X; α is an offset parameter fixed from an auxiliary condition.[43] A major difficulty in using this rule lies on the fact that the number of basis functions scales with X^3, and extrapolations usually require a cardinal number pair as high as $(5,6)$ for the extrapolation. This places severe constraints on the systems that can be treated as well on the used methodologies. For example, it may be argued that enlarging a V5Z wave function may justify the introduction of core-correlation effects as the expected changes are of similar magnitude[46] and so on for higher angular momenta. Such a difficulty is largely overcome by our recently proposed uniform singlet-pair and triplet-pair extrapolation (USTE[43]) method. This assumes the form

$$E_X^{cor} = E_\infty^{cor} + A_3(X+\alpha)^{-3} + A_5(X+\alpha)^{-5} \quad (5)$$

with the constant A_5 related to A_3 via the auxiliary relation $A_5 = A_5^\circ + cA_3^m$, where A_5°, c, and m are "universal" like parameters for a chosen level of theory. For MP2 energies, they are $A_5^\circ = 0.0960668$, $c = -1.582009\ E_h$, and $m = 1$, with $\alpha = -3/8$. Thus, for $m = 1$ (e.g., MP2, and CCSD) and two basis sets X_1 and X_2, one obtains:

$$E_\infty^{cor} = E_{X_2}^{cor} - A_5^\circ(X_2+\alpha)^{-5}$$
$$+ \frac{E_{X_1}^{cor} - E_{X_2}^{cor} + A_5^\circ[(X_2+\alpha)^{-5} - (X_1+\alpha)^{-5}]}{c[(X_2+\alpha)^{-5} - (X_1+\alpha)^{-5}] + (X_2+\alpha)^{-3} - (X_1+\alpha)^{-3}}$$
$$\times [(X_2+\alpha)^{-3} + c(X_2+\alpha)^{-5}]. \quad (6)$$

The above effective two-parameter (E_∞^{cor}, A_3) model has been shown[47] to yield accurate CBS extrapolations of the MP2 correlation energy for a variety of systems, with equally successful results also obtained in CBS extrapolations of raw energies from other theoretical approaches.[43,47–49] We emphasize that the method contains no parameters alien to the theory for which they have been defined, with the coefficients being expected to show only a minor dependence for methods and basis sets that belong to related families. In fact, their "universality" has been explored by showing that accurate results are obtained even for systems that are outside the calibrating set.[38,47,49]

Most recently, we suggested a generalized USTE (GUSTE[44]) scheme. It assumes the form in eq. (5) but with the new auxiliary relation

$$A_5 = \eta A_5^\circ + cA_3^m \quad (7)$$

where η is chosen to impose the calculated $\tau_{53} = A_5/A_3$ ratio. Thus, $\eta_{DTQ} = A_3(\tau_{53}^{DTQ} - cA_3^{m-1})/A_5^\circ$, with the label DTQ implying that

calculations for $X = D - Q$ are used (for generalizations, see Ref. 44). The improvement in the performance originated by GUSTE method relative to other schemes has been documented for more than 20 small systems.[44] Its major advantage lies in the ability to produce accurate CBS extrapolations from raw energies of double zeta (DZ) and TZ quality, a long standing goal.[50] This is important because *ab initio* calculations with larger basis sets that are increasingly more time consuming can be avoided, an essential requirement for this study. Of course, a calculation using a QZ basis set is needed to fix η, but this is done once at a single geometry.[44] Thus, as it will be shown here, the major impact of GUSTE is expected to be in studies of full PESs. Indeed, the GUSTE method should provide high-accuracy CBS extrapolations of PESs calculated with a specific correlated approach at the lowest computational cost possible, while containing enough flexibility to be valid for both ground and excited electronic states.

For the HF energy, a popular CBS extrapolation form is[12] $E_X^{HF} = E_\infty^{HF} + A\exp(-bX)$, where E_∞^{HF}, A, and b are parameters determined from energies for the three largest affordable basis sets. We will use the (T, Q) protocol of Karton and Martin[51] (KM), $E_X^{HF} = E_\infty^{HF} + B/X^{5.34}$. Note that the extrapolations of E_X^{HF} and E_X^{cor} are both geometry-dependent and hence must be performed pointwise. To avoid the huge cost of the QZ calculations using MP2 theory, we could think of combining GUSTE[43] and correlation scaling,[48,52] because this has been shown[48,49] to keep a high accuracy at a lower cost. Unfortunately, MP2 calculations with AVXZ or larger basis sets are unaffordable in low symmetry, thus preventing the use of such a hybrid scheme.

Results and Discussion

Before describing the calculations, a comment on the electronic state is appropriate. Similarly to find the isomer with lowest energy,[16] the spin state that leads to the lowest energy depends on the level of theory and basis set used and requires in principle relaxation of the molecule. Such a treatment can be a heavy computational burden and has not been attempted here. In fact, there is also the issue of chemical unsaturation of C$_{20}$, which can make the electronic state of the title system change even with the geometrical arrangement of the helium atom host at the fullerene. If this is viewed as an open-shell molecule, one could follow Feyereisen et al.[53] and perform open-shell calculations for the state with highest possible spin multiplicity as dictated by Hund's rule. This would imply considering C$_{20}$ in a triplet electronic state. Such an approach would perhaps also be justified for the configurations of HeC$_{20}$ here studied in C_{2v} symmetry, because the fourfold degenerate orbital occupied by the two electrons in C$_{20}$ splits into a_1, a_2, b_1, b_2 orbitals that would possibly remain basically degenerate. However, many of the calculations reported below are for geometries of C_1 symmetry, and such a lowering of symmetry for C$_{20}$ is known to lead to a closed shell ground state.[11] For convenience (no integral-direct implementation of restricted MP2 is available[54]), we have chosen to do all calculations for the singlet state.

All calculations here performed for HeC$_{20}$ have used the Molpro suite of electronic structure programs.[54] They have primarily been carried out for three representative orientations of the He atom relative to the center of the C$_{20}$ structure,[21] which has D_{5d} symmetry.
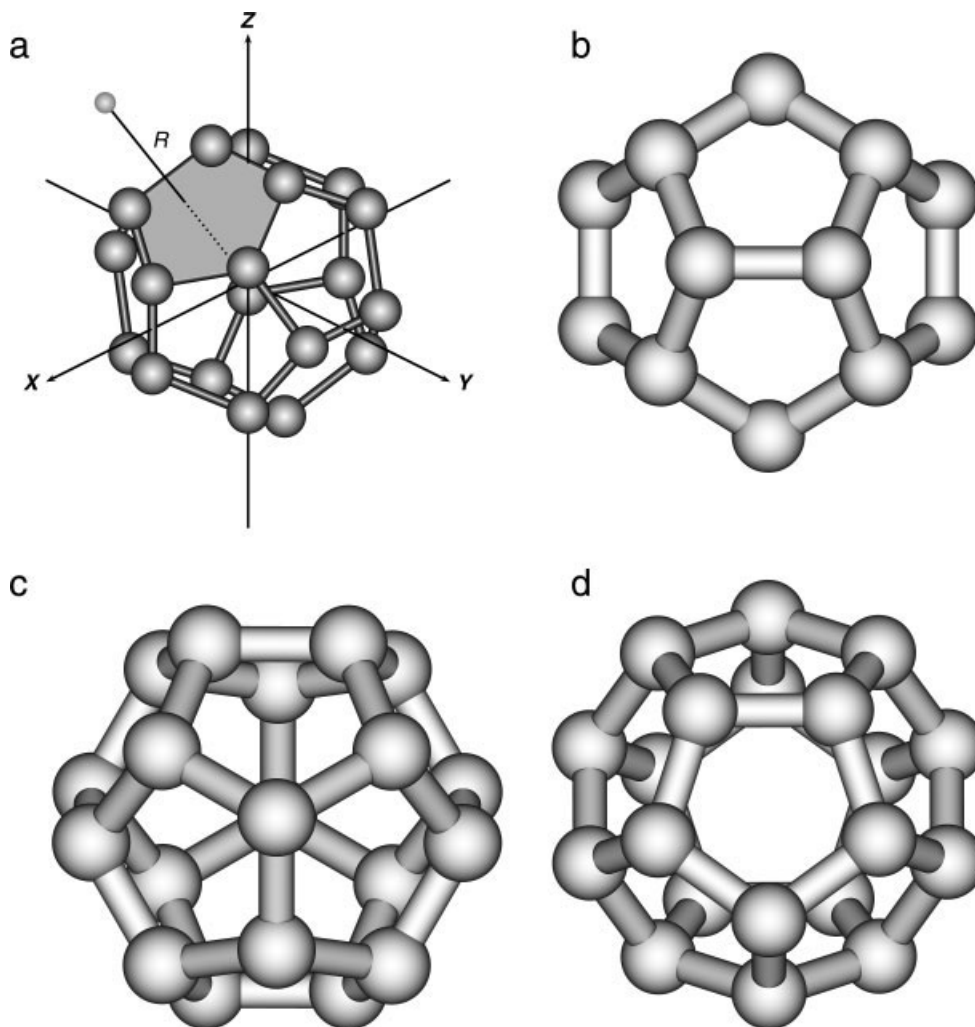
Figure 1. C_{20}–He: (a) structure, with a face of C_{20} in gray, and coordinate system; (b) C_{20} as viewed by the helium atom when attacking the middle of a C–C bond - cut I; (c) as in (b) but attacking a carbon atom—cut II; (d) as in (b) but attacking perpendicularly the center of a pentagonal face—cut III.

The first set of calculations is for He attacking along the z axis (this as well as x and y are C_2 axes of C_{20}) that passes through the center of C_{20} and bisects a C–C bond (cut I). In turn, cut II is for He approaching a carbon-atom site keeping $x = y = z$, whereas, in cut III, it approaches orthogonally to a pentagonal face of the dodecahedron. Panel (a) of Figure 1 shows the adopted coordinate system, whereas panels (b) to (d) illustrate the different cross sections offered by the fullerene to the approaching helium atom. Having set the coordinates in this way, the calculations for cut I may be done in C_{2v} symmetry, whereas the symmetries for cuts II and III have been automatically chosen by Molpro as C_1 and C_s, respectively. Although one might think for numerical consistency of performing all calculations in C_1 symmetry, this would drastically increase its cost. We have then chosen to perform most calculations in the highest allowed symmetry. For example, the calculations for cut I in C_{2v} symmetry allow up to MP2/VQZ calculations to be performed, and hence they have primarily been utilized to calibrate the GUSTE method (i.e., to determine η_{DTQ}). In turn, the calculations in C_1 (or C_s) symmetry

aimed at obtaining an as consistent as possible quantitative picture of the anisotropy of the title interaction. Since the calculations done in C_s symmetry lead essentially to the same result (within a few micro-hartree, < 0.1 meV) at the asymptote* as the ones carried out in C_1, the former symmetry has been utilized whenever viable. Even so, only HF/VQZ or HF/AVQZ calculations could be done in C_s symmetry as the corresponding MP2 ones are too demanding.[†] In fact, this is all that is required, which is clearly an asset of the GUSTE method. Regarding cut II, we have performed calculations

---

*Raw VXZ (AVXZ) energies in E_h at $R = 250$ Å for $X = D, T$, and Q. HF: -759.4196257 (-759.4460812), -759.5743563 (-759.5815216), and -759.6192244 (-759.6218652); MP2: -762.1900688 (-762.2995388), and -762.8594461 (-762.9180337). For the $d_{He} -$ AVXZ basis set, the HF (MP2) energies for $X = D, T$ at $R = 100$ Å are in E_h : -759.4460860 (-762.2995859), -759.5815219 (-762.9180452), and -759.6218660.

[†]Times refer to an Intel Quad core 2.4 MHz processor. At the AVQZ ($d_{He} -$ AVXZ) level, a single SCF cycle costs typically over 15 h (16.5 h).
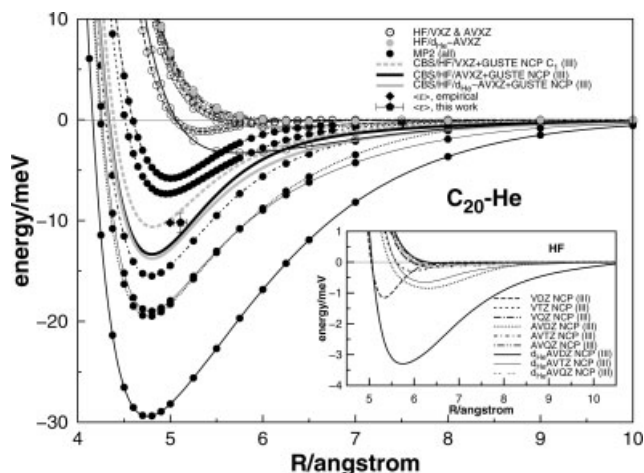
Figure 2. Raw NCP energies (open and solid circles) for the C$_{20}$–He interaction: HF (open black circles, except for the ones corresponding to the largest d_{He}–AVXZ basis set that are shown as gray dots); MP2 (all denoted by black solid dots, with a given line type specifying the basis set). The solid diamond and pentagon with xyerrorbar symbol are the empirical and our estimated spherically averaged estimates; see text. Also shown by the dashed and solid (gray and black) thick lines are the CBS extrapolated curves. The insert highlights the HF curves and their relatively shallow minima (mostly spurious due to BSSE), with the calculated points removed for clarity. Also shown in it are the CBS extrapolated HF curves (note that the CBS extrapolated HF curves are the nearly indistinguishable top curves). The key applies both to the main plot and insert.

in C_1 symmetry as shown in Figure 3. Unfortunately, such calculations are rather expensive even for $X = Q$ at HF level. Thus, they have been performed for all X-tuple zeta basis sets only at HF/VXZ level and for the two smallest basis sets at MP2 level. For DZ and TZ, typically 30 or more geometries have been calculated for cuts I and III (II) over the range $3.5(4.8) \leq R/\text{Å} \leq 250$, whereas for the QZ basis set, only a subset that includes the asymptote has been considered.

To have the capability of describing adequately the vdW well, the wave functions should be able to describe well electric response properties such as the polarizabilities of the interacting fragments. One then expects diffuse functions to play a role. Because these functions are largely missing in VXZ, a set of calculations has been performed whenever affordable with the diffusely augmented aug–cc–pVXZ (or AVXZ) basis set. In addition, calculations using hybrid doubly diffusely augmented correlation consistent basis sets (d-aug-cc-pVXZ for the helium atom and aug-cc-pVXZ ones for the carbon atoms) have also been done. They will be referred heretofore as d_{He}-AVXZ. For brevity, only the NCP interaction energies are shown in Figures 2 and 3, whereas a sample of the raw calculations for cut III is presented in Table 1.

As already noted, the calculations for cut I in C_{2v} symmetry are more economical and have been used with a major twofold purpose: (i) calibrate the GUSTE model; (ii) investigate whether BSSE can be efficiently overcome via CBS extrapolation without CP. Regarding item (ii), the raw data has been first used to obtain E_∞^{cor}, A_3, and A_5 at a reference geometry (arbitrary) here taken as $R = 4.375$ Å. The ratio

$\tau_{53} = A_5/A_3$ has then been calculated and taken[44] as an invariant over the whole PES. Thus, the value so obtained ($\tau_{53} = -1.35981$) has been kept unaltered in all subsequent extrapolations, including those for cut III with basis sets AVXZ and d_{He}–AVXZ. Using such a ratio to define η_{DTQ}, the GUSTE dual-level scheme has then been used to obtain (D, T) correlation energies. These lie typically within a few μE_h of the values based on the rather more expensive (T, Q) extrapolation. In fact, the (D, T) and (T, Q) extrapolated correlation energies are indistinguishable over the whole range of R values here considered. Parenthetically, we observe that a CBS extrapolation with the traditional X^{-3} rule and $\alpha = -3/8$ using (D, T) raw energies underestimate GUSTE for cut I at $R = 5.5$ Å by 173 mE_h, with the underestimation reducing to 24 mE_h if the (T, Q) pair is used. Similar underestimations occur for other cuts and values of R.

To extrapolate the HF energy, we have used both the (T, Q) KM rule and the traditional $(D-Q)$ three-parameter exponential law. For cut I in C_{2v} symmetry, the former yields an unsigned curve nearly parallel to the latter but with an absolute energy lower by 6.02 mE_h, thus predicting interaction energies that differ typically by < 0.3 meV. Compared to the extrapolated HF energy of -759637.13 mE_h at $R = 5$ Å, the error is only $\sim 8 \times 10^{-4}\%$. Alternatively, the HF/VQZ interaction energies may be judged as converged and used as extrapolated ones. In fact, the energies obtained from the KM rule yield interaction HF curves close to the raw QZ ones, and hence our CP curves have been obtained by adding the latter to the GUSTE CP correlation. The CBS extrapolated NCP and CP curves for the VXZ basis set are compared in Figure 4 for cuts I and III, while the NCP ones for cut III obtained with VXZ, AVXZ and $d_{He} - \text{AV}XZ$ basis sets are shown in Figure 2. The agreement between the NCP and CP curves shown in Figure 4 is a clear indication that the BSSE has been largely overcome by CBS extrapolation. The attributes of all extrapolated curves as well as the values of the first two leading dispersion coefficients (dipole–dipole and dipole–quadrupole dispersion interactions) obtained from a least squares fit to the GUSTE correlation energies for intermediate and large distances ($R \geq 6$ Å) using appropriate damping functions[55] are gathered in Table 2. Note
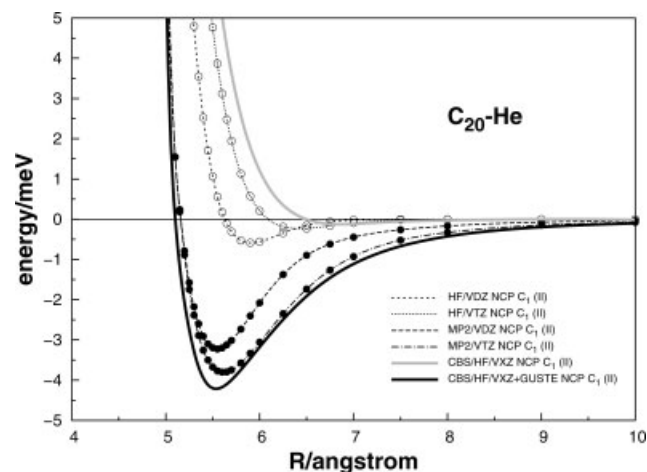

Figure 3. Raw NCP energies and CBS curves for cut II of C$_{20}$–He interaction PES calculated in C_1 symmetry with VXZ ($X = D, T$) basis sets.

Table 1. Sample Raw AVXZ and d_{He}–AVXZ energies[a] for Cut III of C_{20}–He Potential Energy Surface in Hartree.

Basis set	R^d	HF[b]			MP2[c]	
		$X = D$	$X = T$	$X = Q$	$X = D$	$X = T$
AVXZ[e]	4.25	−0.4436471	−0.5789184	−0.6192215	−0.2995564	−0.9178359
	4.5	−0.4449963	−0.5803312	−0.6206431	−0.3001402	−0.9184581
	4.7	−0.4455394	−0.5808979	−0.6212140	−0.3002537	−0.9185942
	5.0	−0.4459197	−0.5812938	−0.6216185	−0.3002131	−0.9185649
	5.25	−0.4460404	−0.5814290	−0.6217585	−0.3001207	−0.9184756
	5.5	−0.4460859	−0.5814884	−0.6218208	−0.3000246	−0.9183830
	6.0	−0.4461097	−0.5815214	−0.6218608	−0.2998638	−0.9182403
	7.0	−0.4461038	−0.5815242	−0.6218668	−0.2996685	−0.9181119
d_{He} − AVXZ[e]	4.25	−0.4437521	−0.5789388	−0.6192264	−0.3000064	−0.9179955
	4.5	−0.4451113	−0.5803527	−0.6206477	−0.3005612	−0.9186039
	4.7	−0.4456602	−0.5809203	−0.6212186	−0.3006636	−0.9187347
	5.0	−0.4460434	−0.5813168	−0.6216234	−0.3006218	−0.9187048
	5.25	−0.4461612	−0.5814512	−0.6217638	−0.3005269	−0.9186164
	5.5	−0.4461998	−0.5815099	−0.6218267	−0.3004198	−0.9185245
	6.0	−0.4462031	−0.5815436	−0.6218656	−0.3002048	−0.9183748
	7.0	−0.4461572	−0.5815364	−0.6218717	−0.2998865	−0.9182017

[a]Calculated in C_s symmetry.
[b]Calculated energies once added a value of 759.
[c]Calculated energies once added a value of 762.
[d]In angstrom.
[e]The energies at the asymptote are given elsewhere.

that C_8 has often large uncertainties, and hence only the leading C_6 coefficient may have quantitative physical meaning. Similarly, the reported (least-squares) error margins should be viewed with caution.

As seen from Figures 2–4, cut III corresponds to the profile with the largest well depth, with similar but shallower curves being predicted for cuts I and II. Figures 2 and 3 (see also Table 1) further show that the HF results saturate fast for basis sets beyond $X = 3$. Because of this and the smaller influence of polarization

Figure 4. NCP and CP CBS curves for the C_{20}–He interaction (cuts I and III) as extrapolated from raw VXZ energies. Shown as impulses in the insert are the (CP–NCP) differences. The CP curves are in dashed.

functions on the HF energy, the extrapolated NCP HF curves are not surprisingly predicted to be rather similar for VQZ and AVQZ, differing from the CP ones only in a tiny well of $\epsilon = (0.08 \pm 0.04)$ meV at $R_m = (6.7 \pm 0.2)$ Å (the $\pm$ sign is chosen such as to encompass the predictions from both basis sets), which is washed out using CP. Although such a feature is generally absent in HF curves for atomic closed shell interactions, C_{20} has permanent electric (quadrupole and higher) moments, and hence the occurrence of a tiny attraction due to induction forces cannot be unexpected. Thus, despite having not done HF calculations with CP for both QZ basis sets due to being highly expensive, we estimate possible inaccuracies in the extrapolated HF curves to be of a fraction of milli electron volt size. A corresponding argument could have been used to estimate the CBS/d_{He} − AVXZ total energy by adding GUSTE/d_{He} − AVXZ to CBS HF/AVXZ. Although Table 1 shows that the differences between the HF/d_{He} − AVXZ and HF/AVXZ curves amount typically to a small fraction of a meV (e.g., 0.1 meV at 5 Å), we have used the extrapolated HF/d_{He} − AVXZ energies. Otherwise, if the HF/AVXZ ones had been used, the value of ϵ for cut III in the seventh entry of Table 1 would be only 0.03 meV shallower.

As expected, the extrapolated VXZ and AVXZ energies yield different interaction curves due to the improved description of polarization effects for the latter. Strikingly though, the well depths of the CBS vdW minima for cut III differ by <3 meV, a small value given the system complexity and quality of basis sets used. To our knowledge, no data are available for comparison with their attributes in Table 2. Because standard calculations with larger basis sets are prohibitive, one should turn for validation to methodologies such as explicitly correlated methods[56] using density fitting.[54,57] This will not be done here. Instead, we will rely on the good results obtained
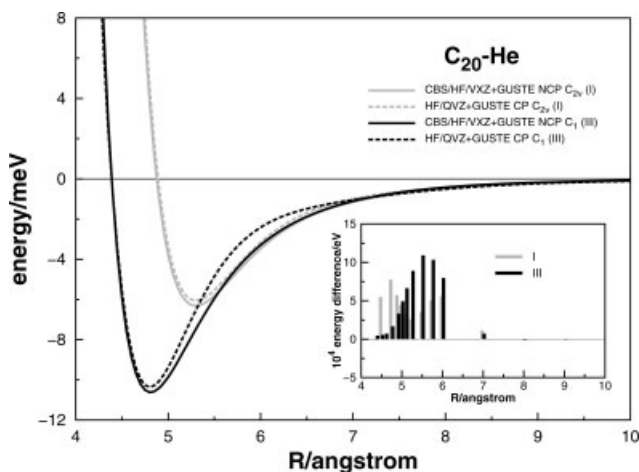
Table 2. Attributes[a] of CBS Extrapolated C$_{20}$ · · · He van der Waals Minima and Fitted Parameters to Long-Range Dispersion.

Cut	basis set	R_m (Å)	ϵ (meV)	$10^{-3} \times C_6^b$ (meV Å^{-6})	$10^{-3} \times C_8^b$ (meV Å^{-8})
I[c]	VXZ	5.30	6.32	60 ± 2	3338 ± 73
	VXZ[d]	5.30	6.06	82 ± 2	1608 ± 87
II[e]	VXZ	5.56	4.21	42 ± 4	4602 ± 189
III[f]	VXZ	4.80	10.62	49 ± 1	3414 ± 38
	VXZ[d]	4.81	10.36	105 ± 1	364 ± 20
	AVXZ	4.80	13.35	162 ± 10	763 ± 406
	d_{He}–AVXZ	4.80	13.76	263 ± 8	229 ± 391

[a] Obtained from a fit of the CBS extrapolated energies to a realistic functional form.[55]
[b] Obtained from a fit of the GUSTE correlation energy to $-\sum_{n=6,8} C_n \chi_n(R) R^{-n}$, where χ_n are dispersion damping functions[55] (with scaling parameter[55] fixed at $\rho = 2.91$ Å).
[c] CBS extrapolation with raw energies calculated in C_{2v} symmetry.
[d] Calculated using CP. Unless indicated otherwise, all entries are NCP.
[e] Raw energies calculated in C_1 symmetry.
[f] Raw energies calculated in C_s or C_1 symmetries.

for small molecules in previous publications[38,43,44,48,49] and compare the predictions here obtained with empirical data. For this, we consider the dependence of the depth of the potential well on the number of carbon atoms, which has been studied for the interaction between two fullerenes.[58] The approach uses a generalization of the method due to Girifalco[59] where the spherically symmetric potential is obtained by treating each fullerene as if it were a sphere with a surface consisting of a uniform density of smeared-out carbon atoms (the C–C intermolecular interactions are represented via a Lennard-Jones (12,6) empirical potential function[58]). Because the radii of both fullerenes are required, the following effective formula is commonly used[58]

$$a_n = a_{60}(n/60)^{1/2} \qquad (8)$$

where n denotes the number of carbon atoms and $a_{60} = 3.55$ Å is the effective radius of C$_{60}$. For the C$_{20}$ dimer, the predicted potential function shows a well depth of $\epsilon = 110.3$ meV at an equilibrium distance of $R_m = 7.0$ Å. In turn, for the much-studied helium dimer,[38,60] one has $\epsilon = 0.949$ meV at $R_m = 2.99$ Å. Use of the popular geometric mean combination rule for ϵ, and arithmetic mean rule for R_m, then yields $\epsilon = 10.2$ meV at $R_m = 5.00$ Å for the C$_{20}$ . . . He spherically averaged interaction. As Figure 2 shows, this empirical value agrees well with the averaged well depth of the NCP results for cuts I–III at AVXZ level, $\langle \epsilon \rangle = 9.8$ meV, if the energy difference (AVXZ–VXZ) in cut III is assumed to be valid also for cuts I and II, which is a fair assumption. Moreover, if the location of the minimum in cut II is associated to the circumradius of the dodecahedron and that of cut III to its inradius, it seems justified to assign a mean value of $\langle R_m \rangle = 5.18$ Å to the corresponding "spherically averaged" vdW equilibrium geometry, a result only 3.6% larger than the above empirical estimate. However, if the midradius (from cut I) and inradius are used instead, the result is 5.05 Å. We resume by suggesting $\langle R_m \rangle = 5.11 \pm 0.7$ Å, thus embracing both estimates. Of course, if corresponding arguments are used for the CBS/d_{He} − AVXZ results, the well depth for the C$_{20}$ . . . He spherically averaged curve will be $\langle \epsilon \rangle = 10.2$ meV at the

same equilibrium distance. From the results for the two largest basis sets, the recommended estimate will then be $\langle \epsilon \rangle = 10.0 \pm 0.2$ meV at $R_m = 5.11 \pm 0.07$ Å. The agreement with the empirical value is now excellent, although an accurate estimate of $\langle \epsilon \rangle$ will require the availability of the full PES, which is outside the scope of this work.

An alternative scheme to estimate the vdW attributes of the spherically averaged C$_{20}$ . . . He interaction consists of using the symmetry properties of dodecahedral fullerene. Because the $z \to x$ (at $\phi = 0°$) and $x \to y$ (at $\theta = 90°$) paths of He are equivalent, one may think of approximating the isotropic interaction simply by the average over the latitudinal angle θ. For this, we have performed calculations over a dense grid of (R, θ) values ($0 \leq \theta/\text{deg} \leq 90$ for $3.5 \leq R/\text{Å} \leq 6$ and $R = 250$ Å in a total of more than 360 points) using the affordable VDZ basis set. The results are displayed as a contour plot in Figure 5, which shows also a smoothed minimum energy path obtained by picking the optimum energy at each value of θ. If one then averages the optimal radii for all θ values, the result is $R_m^D = 5.25$ Å, where the superscript specifies that it has been obtained at the DZ level. Assuming that a contraction of 0.15 Å in the equilibrium bond distance (similar to the one observed for cut III) applies when performing the extrapolation from VDZ to CBS VXZ, one gets $R_m = 5.10$ Å, which lies between the empirical estimate and our own value reported earlier. A further remark to note that the stationary point at $\theta \sim 30°$ is the minimum for attack of the helium atom to the fullerene face (there are 12 others related by symmetry), whereas a very shallow minimum may exist also for the approach to the middle of a C–C bond ($\theta = 90°$). However, this is so tiny ($\ll 0.2$ meV) that one can hardly be sure of its existence with the above grid size and accuracy used. Of course, there will be saddle points connecting those minima as expected from Morse theory for analyzing the topology of a manifold. All such stationary points will replicate along other directions as dictated by the symmetry of dodecahedral C$_{20}$. An estimate of the spherically averaged well depth may also be obtained from Figure 4 but at the expenses of even more drastic approximations. Following a procedure similar to that used above for the intermolecular separation, one obtains $\langle \epsilon \rangle = 4.2$ meV. Because the path shown in Figure 4 intersects cuts
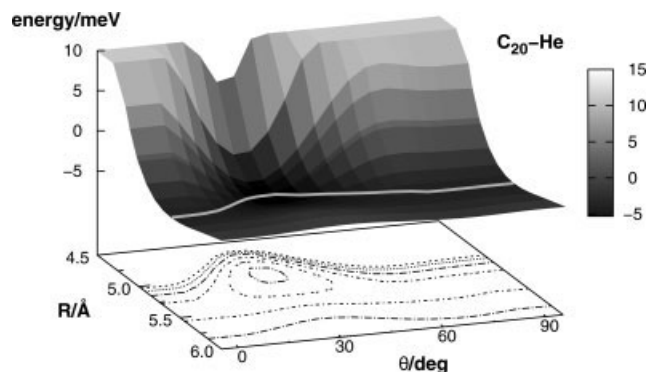
Figure 5. Perspective view of C_{20}–He PES calculated at VDZ level for latitudinal motion of the helium atom along the meridian corresponding to the (x, z) plane. Contours are equally spaced by 1 meV. Also shown by the thick gray line is an approximate minimum energy path: minimum energy at each latitudinal angle.

I and III at the two extrema, one may conjecture that the above well depth translates into its CBS VXZ estimate by the addition of the difference between the CBS and VDZ energies for cut III, that is, by adding a further ~4 meV to get $\langle\epsilon\rangle$ ~8.2 meV. Similarly, we may obtain CBS estimates for the AVXZ and $d_{He} - AVXZ$ basis sets by extracting the necessary energy differences for the cut III from Table 2. This leads in the same order to values of 10.9 and 11.3 meV, which slightly exceed those given above but help on defining a more conservative estimate of $\langle\epsilon\rangle = 10.2 \pm 1$ meV.

We now turn to the fullerene dimer interaction potential, whose averaged well depth may be predicted by using backward the same combination rule. One gets $\langle\epsilon\rangle = 109.6$ meV, a value only 1% smaller than obtained from the Girifalco approach jointly with eq. (8). A simple way to reconcile our predicted vdW attributes for the C_{20} dimer with a Girifalco[59] type potential (based on the same carbon-carbon interaction law) is by using the modified effective radii formula

$$a_n = a_0 + \beta(n/60)^{1/2} \tag{9}$$

where $a_0 = 0.07$ Å and $\beta = 3.48$ Å are fitting parameters determined by imposing the commonly accepted radius of C_{60} fullerene[59] ($a_{60} = 3.55$ Å) and approximately fitting our predicted vdW attributes for the C_{20} dimer (the chosen parameters lead to a well depth of 110.1 meV at $R_m = 7.13$ Å for the C_{20} dimer, thus 10.2 meV at 5.06 Å for C_{20}...He). Although a nonzero radius is predicted for $n = 0$, this is neither surprising due to the empirical nature of eq. (9) nor has practical relevance. Figure 6 compares the potentials so obtained with those predicted using eq. (8). Also shown is a potential energy curve[61] for the dimer of C_{60} that has been obtained by using the local density approximation of DFT and its time-dependent extension. Suffice it to note that the vdW radius here predicted for the C_{20} dimer is considerably larger than the spacing[6] of 4.6 Å in the tightly bound crystal form of this fullerene. Its existence cannot, however, be said to be incompatible with a facile (without an activation barrier) C_{20} coalescence[14, 17] as it refers to an orientationally disordered interaction. Of course, multireference

electronic structure calculations could help in elucidating this issue as a reaction between two closed-shell (partially open[13]) species is being considered.

In summary, Figure 2 and Table 2 show that the NCP CBS/$d_{He} -$ AVXZ vdW attributes agree well with the AVXZ ones, suggesting that the basis set used for the calculation of the raw energies is approaching saturation. Because higher orders of MP perturbation theory and/or use of larger basis sets of the doubly diffusely augmented type for the carbon atoms are too demanding (an AVQZ calculation involves already 2418 primitive atomic orbitals), our CBS/AVXZ NCP results for cut III of $\epsilon = 13.4$ meV at $R_m = 4.8$ Å ($\epsilon = 13.8$ meV at $R_m = 4.8$ Å for CBS/$d_{He} -$ AVXZ) stand as benchmarks. Indeed, CBS extrapolation based on raw energies calculated with the $d_{He} -$ AVXZ basis set predicts a well depth only marginally larger than AVXZ. It appears therefore that a converged estimate of the vdW minimum for He interacting orthogonally to a face center of C_{20} has been obtained. This is impressive as the raw HF and MP2/$d_{He} -$ AVXZ curves show drastic differences from the AVXZ counterparts (for example, the MP2/$d_{He} -$ AVTZ curve lies close to the MP2/AVDZ one and even crosses the latter near $R = 5.5$ Å). Naturally, long-range forces are likely to be best described at the $d_{He} -$ AVXZ level (see, however, ref. 30 for the danger in using large basis sets with high orders of Møller–Plesset perturbation theory), although at the expenses of an enhanced BSSE, which is partly responsible for the stronger attraction at intermediate distances (see the slightly deeper minima in the HF curves shown in Fig. 2). However, it is clear from Figure 4 that BSSE effects have been to a large extent efficiently overcome via CBS extrapolation.

A final remark on CPU times. Except for the GUSTE calibration that requires a single-correlated calculation with the VQZ basis set, the most time-consuming part of the method refers to the HF/VQZ and HF/AVQZ calculations. For example, the cost of a NCP extrapolated point with HF/VQZ+GUSTE(D, T) is 85.7 h (88.9 h for CP), while the HF part itself costs 73.0 h. Thus, the method performs as 1.2 (NCP) to 1.3 (CP) times the HF/VQZ or AVQZ calculations, a performance similar in this context to DFT when using the same basis sets. Although it is known that for large systems MP2 theory
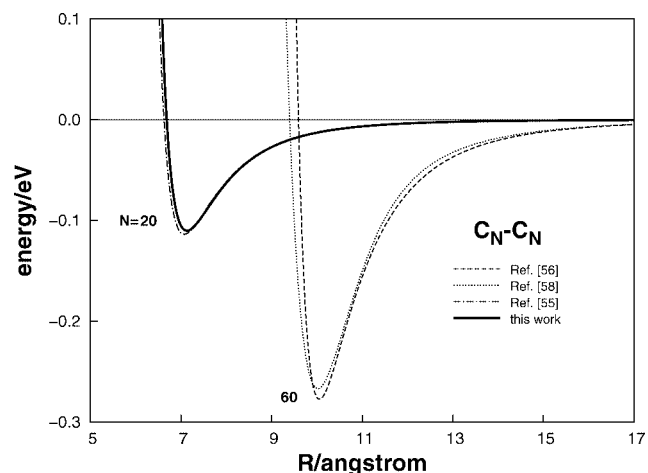

Figure 6. Effective one-dimensional potential curves for the homonuclear dimers of C_{20} and C_{60}.

can be more costly than HF theory, it is also true that significant progress has been made in developing more efficient formulations such as those complemented by density fitting[57] and applying dual basis sets.[62–64] Thus, even if for larger molecular sizes one may reach a break-even point where MP2 starts to dominate (despite MP2 being required here with smaller basis sets than HF), it will be interesting to see in practice how large the system needs to be and one may profit of the above progress.

Conclusions Regarding the Potential of the Method

As already noted, the CBS extrapolated attributes of the He $\cdots$ C$_{20}$ vdW minimum are consistent with those of He $\cdots$ He and C$_{20}$ $\cdots$ C$_{20}$. Thus, although the method will be manageable for studying even larger systems using efficient MP2 methods on modern computer cluster architectures, the attributes of fullerene-dimer interactions can be reliably and cost effectively estimated using the more tractable family of interactions here considered. The results from this work also corroborate previous findings for the helium dimer,[38] suggesting that CBS extrapolation can elude efficiently BSSE while yielding a more accurate PES. This may reveal itself particularly useful in studies involving multiple channels. Although, as already noted, the subject has motivated divided opinions in the literature[32,38–40] (including an almost routine neglect of CP, particularly for open-shell interactions), we have provided (see also Ref. 38) a numerical demonstration that CBS extrapolation works in practice. Finally, the cost of the method for the title system is dominated by the highest-X HF calculation, which suggests that it can be competitive with Kohn-Sham DFT, thus making future comparisons between the two approaches interesting for large systems. Of course, such a cost effectiveness of the method applies to its present form (i.e., using raw MP2 energies), and hence it would be interesting to explore other levels of theory (e.g., by treating electron correlation most efficiently using a coupled cluster[1,24] method). Such an issue is warranted by the performance demonstrated[38,43,44,48,49] thus far for small molecules.

After submission of this work, preliminary calculations for cuts I and III using coupled cluster singles and doubles (CCSD) theory (the gold standard of quantum chemists that scales with basis set size as M^6) have been completed with a VDZ basis set. The calculations give a T_1-diagnostic[65] of $\sim$0.015, suggesting that a CCSD(T) calculation would give results close to the full CI limit. Unfortunately, because all calculations here reported had to be performed integral direct to avoid the bottleneck of storing large quantities of data on disk, no perturbative triple excitations (T) could be included. For the helium atom hosted at a face of dodecahedral C$_{20}$ (cut III), the vdW minimum is found to occur at essentially the same location as in MP2/VDZ but with a well depth of $\epsilon = 4.51$ meV. This is $1.6 - 1.8$ meV (i.e., nearly within our reported uncertainty) shallower than the MP2/VDZ well depth, and about 40% of the difference between the CBS/MP2/VXZ and MP2/VXZ estimates for cut III. An even smaller difference between the MP2 and CCSD results (with the latter being $\sim$1 meV shallower than the former) is observed for the vdW minimum of cut I. Two further observations can be made. First, if the difference between our CBS/MP2 extrapolated estimates and the MP2/VDZ value is added to the raw CCSD/VDZ well depth, one obtains CBS extrapolated CCSD attributes for cut III in very good

agreement with the predictions here reported (see Fig. 3 and Table 2). Second, if a similar difference is conjectured for cut II, then the minimum of the CBS extrapolated CCSD result is likely to fall close to the MP2/VTZ results reported in Figure 3. Of course, adding the (T) correction may enhance the agreement with the MP2 results here reported. Hopefully, the joint use of density fitting approximations with CBS extrapolation may help on providing avenues to explore such issues. Details of the CCSD calculations will be reported elsewhere.

References

1. Helgaker, T.; Jørgensen, P.; Olsen, J. Molecular Electronic-Structure Theory; Wiley: Chichester, 2000.
2. Kohn, W.; Sham, L. Phys Rev A 1965, 140, 1133.
3. Parr, R. G.; Yang, W. Density Functional Theory of Atoms and Molecules; Oxford University Press: New York, 1989.
4. Prinzbach, H.; Weller, A.; Landenberger, P.; Wahl, F.; Wörth, J.; Scot, L.; Gelmont, M.; Olevano, D.; Issendorff, B. Nature 2000, 407, 60.
5. Saito, M.; Miyamoto, Y. Phys Rev Lett 2001, 87, 035503.
6. Wang, Z.; Ke, X.; Zhu, Z.; Zhu, F.; Ruan, M.; Chen, H.; Huang, R.; Zheng, L. Phys Lett A 2001, 280, 351.
7. Prinzbach, H.; Weller, A.; Landenberger, P.; Wahl, F.; Wörth, J.; Scot, L.; Gelmont, M.; Olevano, D.; Issendorff, B. Chem Eur J 2006, 12, 6268.
8. Domene, M. C.; Fowler, P. W.; Mitchell, D.; Seifert, G.; Zerbetto, F. J Phys Chem A 1997, 101, 8339.
9. Lu, X.; Chen, Z. Chem Rev 2005, 105, 3643.
10. An, W.; Gao, Y.; Bulusu, S.; Zeng, X. C. J Chem Phys 2005, 122, 204109.
11. Taylor, P. R.; Bylaska, E.; Weare, J. H.; Kaway, R. Chem Phys Lett 1995, 235, 558.
12. Dunning Jr., T. H. J Chem Phys 1989, 90, 1007.
13. Grimme, S.; Mück-Lichtenfeld, C. Comp Phys Comm 2002, 2, 207.
14. Chen, Z.; Heine, T.; Jiao, H.; Hirsch, A.; Thiel, W.; Schleyer, P. Chem Eur J 2004, 10, 963.
15. Małolepsza, E.; Witek, H. A.; Irle, S. J Phys Chem A 2007, 111, 6649.
16. Sokolova, S.; Lüchow, A.; Anderson, J. B. Chem Phys Lett 2000, 323, 229.
17. Choi, C. H.; Lee, H. Chem Phys Lett 2002, 359, 446.
18. Du, A. J.; Pan, Z. Y.; Ho, Y. K.; Huang, Z.; Zhang, Z. X.; Wang, Y. X. Chem Phys Lett 2001, 344, 270.
19. Ke, X. Z.; Zhu, Z. Y.; S-Zhang, F.; Wang, F.; Wang, Z. X. Chem Phys Lett 1999, 313, 40.
20. Donadio, D.; Colombo, L.; Milani, P.; Benedek, G. Phys Rev Lett 1999, 83, 776.
21. Feyereisen, M. www.ccl.net/cca/data/fullerenes/c20.cart3d.html.shtml.
22. Balasubramanian, K. Chem Phys Lett 1994, 224, 3.
23. Pople, J. A. Rev Mod Phys 1999, 71, 1267.
24. Jensen, F. Computational Chemistry, 2nd ed.; Wiley: Chichester, 2002.
25. Meijer, E. J.; Sprik, M. J Chem Phys 1996, 105, 8684.
26. Johnson, E. R.; Becke, A. D. J Chem Phys 2005, 123, 024101.
27. Grimme, S. J Comput Chem 2006, 27, 1787.
28. Jurečka, P.; Cerny, J.; Hobza, P.; Salahub, D. R. J Comput Chem 2006, 28, 555.
29. Furche, F.; Burke, K. Ann Rev Comp Chem 2005, 1, 19.
30. Olsen, J.; Christiansen, O.; Koch, H.; Yørgensen, P. J Chem Phys 1996, 105, 6082.
31. van Duijneveldt, F. B.; van Duijneveldt-van de Rijdt, J. G. C. M.; van Lenthe, J. H. Chem Rev 1994, 94, 1873.
32. Halkier, A.; Klopper, W.; Helgaker, T.; Jørgensen, P.; Taylor, P. R. J Chem Phys 1999, 111, 9157.
33. Lee, J. S.; Park, S. Y. J Chem Phys 2000, 112, 10746.
34. Dunning Jr., T. H. J Phys Chem A 2000, 104, 9062.

35. Brutschy, B.; Hobza (eds.), P. Chem Rev 2000, 100, 3861.
36. Barrientos, C.; Sordo, J. A. Theor Chem Acc 2007, 118, 733.
37. Boys, F.; Bernardi, F. Mol Phys 1970, 19, 553.
38. Varandas, A. J. C. Theor Chem Acc 2008, 119, 511.
39. Boese, A. D.; Oren, M.; Atasoylu, O.; Martin, J. M. L.; Kállay, M.; Gauss, J. J Chem Phys 2004, 120, 4129.
40. Schwenke, D. W.; Truhlar, D. G. J Chem Phys 1985, 82, 2418.
41. Schwartz, C. Phys Rev, 1962, 126, 1015.
42. Kutzelnigg, W.; Morgan III, J. D. J Chem Phys 1992, 96, 4484.
43. Varandas, A. J. C. J Chem Phys 2007, 126, 244105.
44. Varandas, A. J. C. J Phys Chem A 2008, 112, 1841.
45. Helgaker, T.; Klopper, W.; Koch, H.; Noga, J. J Chem Phys 1997, 106, 9639.
46. Peterson, K. A.; Wilson, A. K.; Woon, D. E.; Dunning Jr., T. H. Theor Chem Acc 1997, 97, 251.
47. Varandas, A. J. C. Phys Scripta (Comm At Opt Mol Phys), 2007, 76, C28.
48. Varandas, A. J. C. Chem Phys Lett 2007, 443, 398.
49. Varandas, A. J. C. J Chem Phys 2007, 127, 114316.
50. Truhlar, D. G. Chem Phys Lett 1998, 294, 45.
51. Karton, A.; Martin, J. M. L. Theor Chem Acc 2006, 115, 330.
52. Varandas, A. J. C.; Piecuch, P. Chem Phys Lett 2006, 430, 448.
53. Feyereisen, M.; Gutowski, M.; Simons, J. J Chem Phys 1992, 96, 2926.
54. Werner, H.-J.; Knowles, P. J.; Lindh, R.; Schütz, M.; Celani, P.; Korona, T.; Manby, F. R.; Rauhut, G.; Amos, R. D.; Bernhardsson, A.; Berning, A.; Cooper, D. L.; Deegan, M. J. O.; Dobbyn, A. J.; Eckert, F.; Hampel, C.; Hetzer, G.; Lloyd, A. W.; McNicholas, S. J.; Meyer, W.; Mura, M. E.; Nicklass, A.; Palmieri, P.; Pitzer, R.; Schumann, U.; Stoll, H.; Stone, A. J.; Tarroni, R.; Thorsteinsson, T. Molpro, version 2002.6, a package of ab initio programs, 2003. See http://www.molpro.net.
55. Varandas, A. J. C. Adv Chem Phys 1988, 74, 255.
56. Klopper, W.; Manby, F. R.; Ten-No, S.; Valeev, E. F. Int Rev Phys Chem 2006, 25, 427.
57. Werner, H.; Manby, F.; Knowles, P. J Chem Phys 2003, 118, 8149.
58. Zubov, V. I. Fullerenes, Nanotubes, Carbon Nanostruct 2004, 12, 499.
59. Girifalco, L. A. J Phys Chem 1992, 96, 858.
60. Cencek, W.; Jeziorska, M.; Bukowski, R.; Jaszuński, M.; Jeziorski, B.; Szalewicz, K. J Phys Chem A 2004, 108, 3211.
61. Pacheco, J. M.; Ramalho, J. P. P. Phys Rev Lett 1997, 79, 3873.
62. Woliński, K.; Pulay, P. J Chem Phys 2003, 118, 9497.
63. Ishimura, K.; Pulay, P.; Nagase, S. J Comput Chem 2006, 27, 407.
64. Steele, R. P.; DiStasio, R. A.; Shao, Y.; Kong, J.; Head-Gordon, M. J Chem Phys 2006, 125, 074108.
65. Lee, T. J.; Taylor, P. R. Int J Quantum Chem, 1989, S23, 199.